On the measurement of turbulence energy dissipation in stirred vessels with PIV techniques

S. Baldi, D. Hann and M. Yianneskis

Experimental and Computational Laboratory for the Analysis of Turbulence
Division of Engineering
King's College London
Strand, London WC2R 2LS, U.K.

ABSTRACT

The mean flow and turbulence fields and the turbulence energy dissipation rate in a vessel stirred by a hydrofoil impeller were analysed using the two-dimensional Particle Image Velocimetry (PIV) technique. The vessel diameter was $T = 100$ mm and was stirred by an impeller of diameter $D = T/3$, rotated at a speed of 2,165 r.p.m. to achieve a Reynolds number of 40,000 and ensure fully-turbulent flow in the vessel. The measurements were made with a 2-D PIV system comprising a PCO Sensicam SVGA camera and Nikon 55 mm lenses. The light from a 3W Argon laser was used to generate a light sheet with a fibre optic and a cylindrical lens fibre module. Measurements were performed for different spatial resolution configurations. In order to assess the accuracy of these measurements and of the PIV technique itself, the results were compared to the data obtained in the same vessel configuration with the LDA technique by Fentiman *et al.* (1998). The entire flow field in the vessel as well as smaller areas in the discharge stream region below the impeller were analysed. Particular attention is given to the effect, potential and limitation of spatial resolution on the estimation of energy dissipation. The energy dissipation was estimated using the direct definition, i.e. evaluating the instantaneous spatial gradients of the Reynolds stresses. Other methods available in literature were considered as well and the results compared. The effects of number of samples employed in the ensemble-averaging over the energy dissipation estimation was considered as well. The experiments show good agreement with many findings from other works on the analysis of turbulence properties and energy dissipation in stirred vessels. Moreover the performance of PIV in the turbulence energy dissipation estimation was found to be very similar to other earlier studies.

1. INTRODUCTION

Stirred vessels are employed in around 25% of all process engineering operations. The determination of the distribution of the dissipation rate of the turbulence kinetic energy (ε) is of paramount importance for the optimisation of fluid mixing processes in such vessels. Knowledge of the maximum and minimum values of ε and of its distribution in the impeller stream and bulk flow in the vessel is required to ensure that processes such as break-up of drops, particles and bubbles in liquid-liquid, solid-liquid and gas-liquid mixing respectively are achieved and the desirable product quality is obtained. Although a large amount of information has already been obtained on the mean flow and turbulence levels in stirred tanks with LDA and other methods (see, for example, Yianneskis et al., 1987, Schaefer et al., 1998, Yianneskis and Whitelaw, 1993), the measurement of the dissipation rate remains a challenging task, primarily in view of the small scales at which dissipation takes place. Consequently, most approaches employed to date for the determination of ε have made use of approximate relations, assuming local isotropic turbulence and equations of the general form (Kresta, 1998):

$$\varepsilon = A \, u'^3/L \tag{1}$$

where A is a constant, u' the turbulence level in the main flow direction and L a characteristic length scale, often assumed to be a tenth of the impeller diameter (D). Clearly, such approaches assume that the length scale is constant throughout the vessel and that many terms contributing to the energy dissipation equation are negligible. Although the above relation may yield approximate volume-averaged energy dissipation values, such results can be misleading, as both assumptions are of limited validity and better ways to determine ε accurately are necessary. Jaworski and Fort (1991) applied a mechanical energy balance of the moving liquid to small volumes in order to estimate the local energy dissipation. Wernersson and Tragardh (1999) estimated the energy dissipated in stirred vessels using a method based on Kolmogorov's spectrum hypothesis that if the local Reynolds number is large enough, the local energy dissipation can be estimated from the slope of the energy spectrum (see Pope, 2000). Stoots and Calabrese (1995) calculated an approximation of the energy dissipation using the deformation rates given by mean velocity gradients. Other methods imply dimensional assumptions (Hinze, 1975):

$$\varepsilon = 15\nu \frac{u'^2}{\lambda^2} \tag{2}$$

where ν is kinematic viscosity, λ is the microscopic turbulence length scale and u' is the rms velocity in the main flow direction; or

$$\varepsilon = A' \frac{q^{3/2}}{L} \tag{3}$$

where A' is an empirical constant, L is the integral length scale and q is the turbulent kinetic energy. Many others have employed turbulence power spectrum methods based on the following equation which is valid for isotropic turbulence:

$$\varepsilon = 15\nu \int \kappa_1^2 E_1(\kappa_1) d\kappa_1 \tag{4}$$

where $E_1(\kappa_1)$ is the one-dimensional power spectrum and κ is the wave number. Lee and Yianneskis (1998) evaluated the energy dissipation in the impeller stream of a Rushton turbine using both relations:

$$\varepsilon = \frac{0.85 k^{3/2}}{(3\Lambda_x^2)^{1/2}} \tag{5}$$

$$\varepsilon = \frac{(\overline{u'^2})^{3/2}}{\Lambda_x} \tag{6}$$

where k is the turbulence kinetic energy, u' is the mainstream rms velocity and Λ_x is the integral length scale.

The PIV technique allows for a totally different approach in calculating the energy dissipation. Instantaneous velocity data in adjacent points in space are available from PIV analysis, thus permitting the

direct calculation of turbulence energy dissipation through the determination of the instantaneous velocity gradients. Sheng *et al.* (2000) developed a large eddy PIV method for dissipation rate estimation, based on a dynamic equilibrium assumption between the spatial scale that can be resolved by PIV and the sub-grid scales. Sharp *et al.* (1998) studied the effects of isotropic assumptions and spatial resolution in PIV over the estimation of ε around a Rushton turbine. Piirto *et al.* (2000) and Saarenrinne *et al.* (2001) analysed the correlation between energy dissipation, spatial resolution and length scales using PIV. It should be noted here that none of the aforementioned works has reported the distribution of ε across a stirred vessel in fully turbulent flow based on direct measurement of the instantaneous velocity gradients.

2. FLOW CONFIGURATION, INSTRUMENTATION AND TECHNIQUES

A standard configuration cylindrical vessel of diameter T = 100 mm was used in this study. The vessel was equipped with four equi-spaced wall mounted baffles of width B = 0.1T; the liquid column height was H = T. The vessel was constructed from acrylic plastic (Perspex) and was located inside a square acrylic container filled with distilled water in order to minimize the refraction of the laser sheet over the outer cylindrical surface of the vessel. The vessel was filled with distilled water seeded with 10 μm-sized hollow silver coated glass spheres with a density of the order of 1000 kg/m^3 (same as water). The vessel was located on a base plate that allowed movement in the vertical and the two horizontal directions in order to ease the calibration procedures of the PIV system. The impeller used was a three-bladed hydrofoil axial impeller with a diameter of D = T/3 described in detail by Fentiman *et al.* (1998). A transparent acrylic lid was positioned in the vessel, at a height equal to the liquid column height H, in order to prevent entrainment of air bubbles into the flow from the free surface of the liquid. Measurements were taken at an impeller rotational speed of 2165 rpm corresponding to a Reynolds number (Re) of 40000 and to a tangential velocity at the tips of the blades V_{tip} = 3.78 m/s. The origin of the coordinates system used is the centre of the base of the vessel with $\overline{U}_z$, $\overline{U}_r$ and u_z', u_r' referring to the mean and root-mean-square (r.m.s.) velocities in the axial (z) and radial (r) coordinates direction respectively.

An OFS PIV system was employed for the experiments. An Argon-ion laser provided the light sheet. A timing box by OFS was used to trigger a Sensicam digital camera and a Bragg cell that produced the laser pulses. The pulsing laser illuminated a thin vertical sheet passing through the centre of the vessel and midway between two baffles (in the θ= 0° plane). The axial and radial velocity components were measured.

For each set of measurements 500 pairs of pictures were taken. The picture pairs were grabbed at a frequency between 1 and 2 Hz, according to the camera limitations and the resolution employed. The resolution of the camera was changed according to the size of the area on which measurements were taken: it was increased from 13 pixels/mm (lowest spatial resolution) to 72 pixels/mm (highest spatial resolution). In the lowest resolution case the area covered by the camera picture was the entire vessel, while in the highest resolution case it comprised an area 10 mm wide and 3.5 mm high just below the impeller region. Considering an image resolution varying from 13 to 72 pixels/mm depending on the image size, an almost negligible time uncertainty, a software interpolation accuracy of 0.1 pixels and a calibrating mapping accuracy of 1 pixel, the error in the velocity measurements was found to vary from 3.7 – 6 % of V_{tip}. Each interrogation cell comprised 64x64 pixels with an overlapping of 32 pixels for the cross correlation processing step, 32x32 pixels with an overlapping of 16 pixels for the subsequent adaptive cross correlation processing step and, when necessary, 16x16 pixels with an overlapping of 8 pixels for the last adaptive cross correlation step.

3. RESULTS

3.1 Mean flow and turbulence fields

The ensemble averaged mean flow and turbulence fields across the whole vessel were analysed over an image area that covered the plane illuminated by the laser sheet, that is: r/T = 0.0 - 0.5 and z/T = 0.0 - 0.7. The resolution of the camera was 13 pixels/mm. The quantities that were derived from the analysis of these

data are the ensemble-averaged mean velocity, the corresponding r.m.s. velocity, skewness and kurtosis, as well as the Reynolds stresses.

In Figure 1 the velocity vector map showing the whole flow field along a plane over half of the vessel is presented. A reference vector representing a velocity of 0.1 V_{tip} is also shown. Each vector represents an interrogation cell. The outline of the impeller and the shaft is also shown in each figure. The impeller generates a main vortical motion, which occupies most of the vessel. The maximum velocity is 0.26 V_{tip} and is located just below the impeller. In the region z/T < 0.1 and r/T < 0.13 a small counter-rotating vortex can be noted, which rotates in clockwise direction. The r.m.s. velocity analysis revealed that, as expected, the most turbulent areas were located along the edge of the impeller stream region under the impeller and were characterised by values of u_z' a little higher than 0.1 V_{tip}. The centre discharge region, on the contrary, presents low axial rms values. The radial turbulence level was analysed as well and found to be higher along the edge of the main discharge stream as well and also close to the base of the vessel.

The skewness, the kurtosis and the Reynolds stresses were analysed as well. The main axial discharge stream was found to be characterised by a large positive skewness and a high kurtosis. Large negative values of skewness and high values of kurtosis were noticed along the edges of the main discharge stream. These results are very similar to the ones obtained, using the LDA technique, by Fentiman *et al.* (1999) with the same impeller and under the same conditions.

In order to estimate the accuracy of 2-D PIV measurements, the results obtained were compared to the results obtained with the same impeller and vessel with the LDA technique by Fentiman *et al.* (1998). Figures 2 (a) and (b) show some of the results obtained from these comparisons. The axial mean velocity and the axial r.m.s. velocity in the region below the impeller are shown. The graphs show very good agreement between the data obtained with PIV and those obtained with LDA. Results for other z/T values showed similar agreement. The analysis of the radial mean and r.m.s. velocities produced results very similar to the axial velocity ones.

Conclusively the data obtained with PIV measurements are very similar to those obtained with the LDA technique, and in most locations the differences are within the measurement errors. Therefore the PIV technique with the set up used proved to be very reliable.

3.2 Turbulence energy dissipation

PIV techniques can be used to measure the gradients of the Reynolds stresses comprising the main unknowns in the ε equation (7) (Sharp et al., 1998), provided that such gradients can be measured over volumes sufficiently small and comparable to the Kolmogorov scales.

$$\varepsilon = \nu \left\{ \begin{array}{l} 2\left(\overline{\left(\dfrac{\partial u_i}{\partial x_i}\right)^2} + \overline{\left(\dfrac{\partial u_j}{\partial x_j}\right)^2} + \overline{\left(\dfrac{\partial u_k}{\partial x_k}\right)^2} \right) + \\[3mm] + \overline{\left(\dfrac{\partial u_i}{\partial x_j}\right)^2} + \overline{\left(\dfrac{\partial u_j}{\partial x_i}\right)^2} + \overline{\left(\dfrac{\partial u_i}{\partial x_k}\right)^2} + \overline{\left(\dfrac{\partial u_k}{\partial x_i}\right)^2} + \overline{\left(\dfrac{\partial u_j}{\partial x_k}\right)^2} + \overline{\left(\dfrac{\partial u_k}{\partial x_j}\right)^2} + \\[3mm] + 2\left(\overline{\dfrac{\partial u_i}{\partial x_j}\cdot\dfrac{\partial u_j}{\partial x_i}} + \overline{\dfrac{\partial u_i}{\partial x_k}\cdot\dfrac{\partial u_k}{\partial x_i}} + \overline{\dfrac{\partial u_j}{\partial x_k}\cdot\dfrac{\partial u_k}{\partial x_j}} \right) \end{array} \right\} \qquad (7)$$

where u is the fluctuating velocity, the subscripts i, j, k denote the three Cartesian directions and ν is the kinematic viscosity. As the measurements were taken using a two-dimensional PIV system, only two velocity components (u_r and u_z) and therefore 5 terms in the full twelve-term turbulent dissipation energy equation terms were available. For this reason the unknown terms were assumed to be statistically isotropic and thus derivable from the known ones (see Sharp *et al.*, 1998). Fentiman *et al.* (1999), who studied, using an LDA technique, the same system that is the object of this work, found the differences between radial and tangential rms velocities in different regions of the vessel to be very small and it may therefore
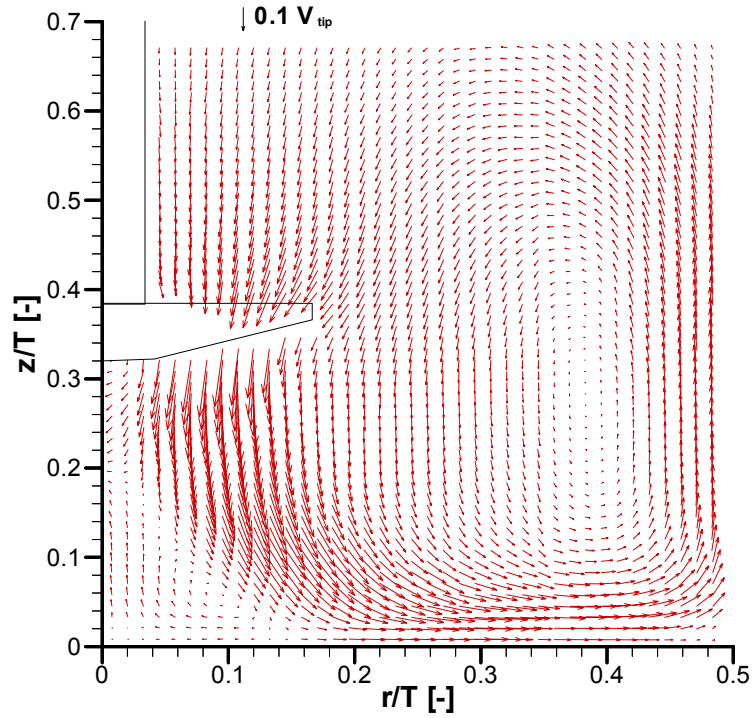
Figure 1 - 360° ensemble-averaged velocity vector map in θ= 0° plane.

a)

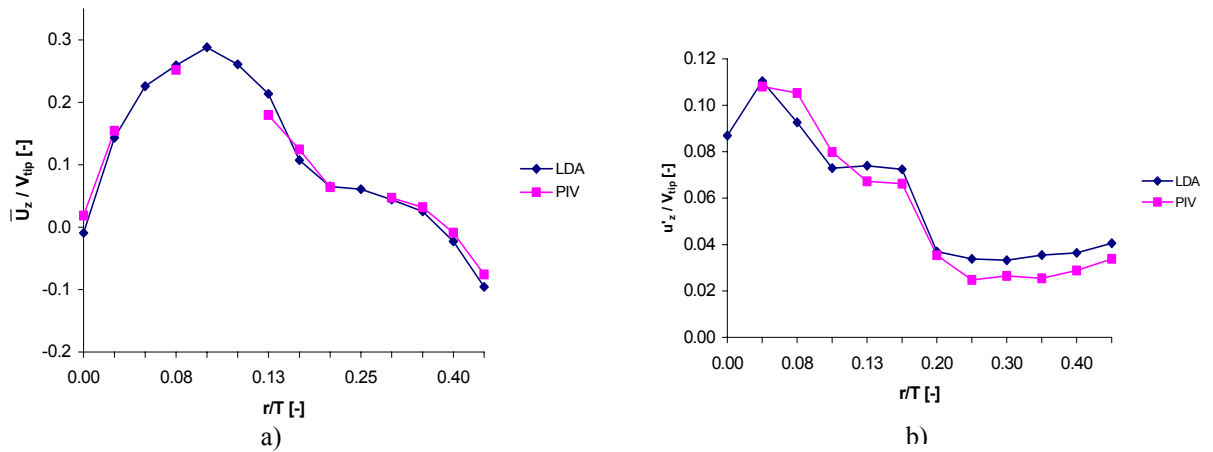b)

Figure 2 - a) - Comparison of $\overline{U}_z/V_{tip}$ values in the plane z/T = 0.28 obtained by Fentiman et al. (1998) with LDA and in present work with PIV.

b) - Comparison of u'_z/V_{tip} values in the plane z/T = 0.18 obtained by Fentiman et al. (1998) with LDA and in present work with PIV.

be expected that the assumption of statistical isotropy is acceptable in the present two-dimensional PIV analysis, appreciating nevertheless that the results are affected by these approximations. Therefore, in order to estimate the turbulence energy dissipation, the 7 missing terms were evaluated by considering

turbulence as statistically isotropic and thus using relations (8a-c) below (see Sharp *et al.*, 1998) derived from the conditions of isotropy equations (see Hinze, 1975):

$$\overline{\left(\frac{\partial u_\varphi}{\partial \varphi}\right)^2} = \frac{1}{2}\left(\overline{\left(\frac{\partial u_r}{\partial r}\right)^2} + \overline{\left(\frac{\partial u_z}{\partial z}\right)^2}\right) \tag{8a}$$

$$\overline{\left(\frac{\partial u_r}{\partial \varphi}\right)^2} = \overline{\left(\frac{\partial u_\varphi}{\partial r}\right)^2} = \overline{\left(\frac{\partial u_z}{\partial \varphi}\right)^2} = \overline{\left(\frac{\partial u_\varphi}{\partial z}\right)^2} = \frac{1}{2}\left(\overline{\left(\frac{\partial u_r}{\partial z}\right)^2} + \overline{\left(\frac{\partial u_z}{\partial r}\right)^2}\right) \tag{8b}$$

$$\overline{\frac{\partial u_r}{\partial \varphi}\cdot\frac{\partial u_\varphi}{\partial r}} = \overline{\frac{\partial u_z}{\partial \varphi}\cdot\frac{\partial u_\varphi}{\partial z}} = \left[\frac{\left(-\frac{1}{2}\overline{\left(\frac{\partial u_r}{\partial r}\right)^2}\right)+\left(-\frac{1}{2}\overline{\left(\frac{\partial u_z}{\partial z}\right)^2}\right)}{2}\right] = \tag{8c}$$

$$= -\frac{1}{4}\left(\overline{\left(\frac{\partial u_r}{\partial r}\right)^2} + \overline{\left(\frac{\partial u_z}{\partial z}\right)^2}\right).$$

Where φ indicates the tangential direction. Consequently the expression for ε becomes:

$$\varepsilon = \nu\left\{2\overline{\left(\frac{\partial u_r}{\partial r}\right)^2} + 2\overline{\left(\frac{\partial u_z}{\partial z}\right)^2} + 3\overline{\left(\frac{\partial u_r}{\partial z}\right)^2} + 3\overline{\left(\frac{\partial u_z}{\partial r}\right)^2} + 2\overline{\frac{\partial u_r}{\partial z}\cdot\frac{\partial u_z}{\partial r}}\right\} \tag{9}$$

As the PIV technique calculates the velocity data averaging over an interrogation cell, the spatial resolution of the data is very important. The experiments were therefore performed paying particular attention to the resolution effects.

Figure 3 shows ε results obtained with 1.25 mm resolution. Results over half of the vessel are displayed. The $\dfrac{\varepsilon}{N^3 D^2}$ values range from 0 to 0.02. Two highly turbulent regions are evident in the region just below the impeller. The remainder of the impeller stream presents lower values. The bulk of the vessel, as expected, is characterised by very low energy dissipation. Nevertheless as this area covers most of the vessel volume, its contribution to the total energy dissipation is rather large. In order to validate the results an integration of ε over the whole vessel was performed, the result of which could be compared with the power number of the impeller used. The power number was analysed by Fentiman *et al.* (1998) and was found to be 0.22. From the integration a power number corresponding to about 7 % of the measured power number was found. It should be noted that this value is about two times higher than that obtained with a spatial resolution of 2.5 mm. The result is in agreement with Piirto *et al.* (2000) and Saarenrinne *et al.* (2001) who found out that the measured ε increased with increasing spatial resolution of the PIV measurements. Lack of resolution of the dissipative scales was clearly the most likely reason for this important discrepancy.

Experiments were then performed with smaller spatial resolutions. In order to obtain high resolution, the camera had to be focused on an image area smaller than for the previous cases. With a spatial resolution of 0.285 mm, values of ε 10 times higher than those obtained with the previous case (1.25 mm resolution) were found. As the results covered only a small area of the vessel, estimation of the integrated value of ε and the consequent comparison with the power number were not possible. Extensive data analysis showed that, as might be expected, increasing resolution does not produce a similar or proportional increment in the ε values across the vessel: the highest and the lowest ε values are affected in different way. Therefore, in order to assess the ε results, measurements were performed at higher resolutions and the variation of ε with spatial resolution was studied and compared with previously reported studies. Measurements were performed with spatial resolutions of 0.444 mm, 0.222 mm and 0.111 mm.

6

From earlier estimation of the average Kolmogorov length scale from the power number, a value η = 37 μm was found; this means that the resolution of 0.111 mm is about 3 times the average η. Nevertheless it should be noted that the smallest Kolmogorov length scale, as it can be deduced by its definition $(\eta = (v^3/\varepsilon)^{0.25})$, is located in regions where ε is highest. Therefore the smallest η value in the vessel should be less than 37 μm. The results obtained from the 0.111 mm spatial resolution measurements are shown in Figure 4.
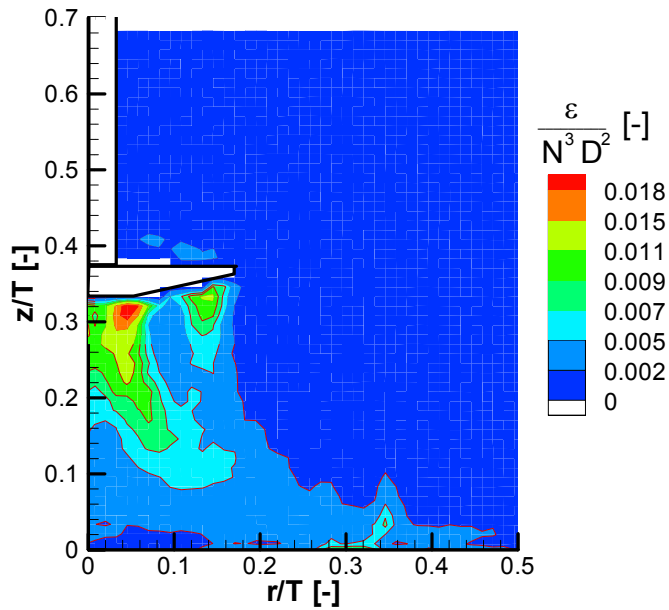
Figure 3 - Contour plot of the normalised turbulence energy dissipation; spatial resolution: 1.25 mm.
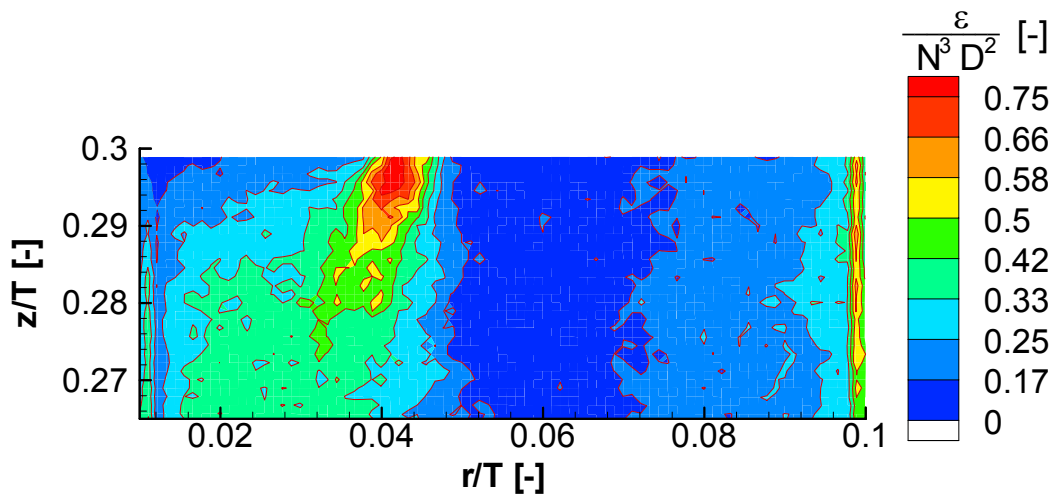
Figure 4 - Contour plot of the normalised turbulence energy dissipation; spatial resolution: 0.111 mm.

An increase in the measured values of ε in comparison to the results of Figure 3 (1.25 mm resolution) can be noted, mostly in the region where turbulence is highest. There, the dissipation value is about 40 times greater than the previous case. Values about 80 and 8 times the mean dissipation value, $\bar{\varepsilon} = 0.54$ m^2/s^3, were found in the highest and lowest turbulence regions respectively; very similar values were found by Cutter (1966) and Zhou and Kresta (1996b) in a vessel stirred by a pitched blade turbine. Lee and Yianneskis (1998) studying the turbulence properties of the impeller stream of a Rushton turbine found a maximum value of the non-dimensional energy dissipation around 20. This value is about 25 times the maximum value found in this experiment ($\varepsilon^* = 0.8$), the same ratio that relates the power numbers of the Rushton ($P_o \cong 5.5$) and the hydrofoil impellers ($P_o \cong 0.22$). Considering the highest dissipation value from Figure 4, $\varepsilon = 0.75*N^3D^2 = 39$ m^2/s^3, a value about 13 μm is found for η. This implies that the present resolution is about 8.5 times the smallest turbulent length scale. The Taylor spatial microscales were analysed as well and values around 0.5 mm were found in the highest turbulence region below the impeller.

The energy dissipation has often been estimated using the dimensional analysis relation expressed in equation (1). This relation is applicable only to flows or regions where the turbulence is homogeneous and isotropic. Moreover, as the length scale varies substantially according to the turbulence level in different regions of the vessel, a single value for L cannot describe such a complex flow. Nevertheless equation (1) has often been used and suggested by various authors (see, for example, Kresta and Wood, 1993, Zhou and Kresta, 1996a) in order to estimate turbulence dissipation in even complex and fully three-dimensional flows. These estimates of turbulence energy dissipation do not take in consideration the contribution given by rms velocity components other than that in the main flow direction. For comparative purposes the data concerning turbulence levels obtained by the PIV analysis and described in the previous paragraphs were used to make an estimation of turbulence dissipation according to equation (1). The resulting contours of normalised ε are shown in Figure 5. Considering the impeller stream region, where the highest resolution measurements are available from this work, it can be noted that the highest dissipation values are rather different. In Figure 4 the highest values are around 0.41 while in Figure 5 values around 0.75 are observed. Moreover, in order to assess the ε values obtained with equation (1), they were integrated over the whole vessel volume. The integration produced a value of $P_o = 0.265$, about 20 % higher than the real power number. It should be noted that, even though this value is not far from P_o, equation (1) presents some approximations, which are pointed out below, that produce an incorrect ε local distribution. Considering Figures 3 and 5 some considerations must be made. Both plots show ε values obtained from 1.25 mm resolution experiments; nevertheless ε distribution shapes are rather different. The energy dissipation obtained with equation (1) (Figure 5) presents high values ($\varepsilon^* > 0.4$) in a large region contained in $0.07 < z/T < 0.25$ along the border of the main axial stream below the impeller. The energy dissipation calculated with the direct definition (see Figure 3) shows a ε distribution more regular with values decreasing with the distance from the impeller. This distribution seems more likely and, furthermore, it was obtained from the direct calculation of ε (equation (9)). Sheng *et al.* (2000), studying turbulence dissipation in a vessel stirred by a pitched blade turbine, found similar results: they obtained an ε distribution very similar to the one obtained in this work (Figure 3). Moreover, estimating ε over the whole vessel using a large eddy PIV method, they found that the dissipation rate obtained by dimensional analysis (like, for example, equation (1)), has much larger values in the bulk of the vessel than those found by large eddy approach, which is based on the ε definition employed in this work. Therefore it can be concluded that ε estimation through equation (1) produces results that are reliable if the average energy dissipation and its integration over the vessel is considered, but are rather incorrect when local ε values and distribution are estimated.

Figure 6 shows the effect of the spatial resolution on the measurements of the turbulence energy dissipation in this work. The data shown in the graphs represent the spatial average over a small area located just below the impeller in the most turbulent region. Six different spatial resolutions were considered for the energy dissipation: 2.5 mm, 1.25 mm, 0.444 mm, 0.285 mm, 0.222 mm and 0.111 mm. The influence of spatial resolution is thought to be due to the strong dependence of the velocity gradients estimation on the distance between two adjacent vectors. The estimates of energy dissipation show small differences at low spatial resolutions (high dx) while they differ significantly at high resolutions (low dx). In the latter case, a small change in the spatial resolution produces strong variations in the value of the estimated ε.

8

Observing Figure 6 it can be noted that the strong change in ε values occurs for resolutions smaller than about 0.5 mm. In this region a decrease in interrogation cell size, and thus a reduction of the distance dx between adjacent vectors, of 50 % from 0.444 mm to 0.222 mm, produces an increase in the estimated ε value of up to 250 %. The Taylor microscales were analysed as well and were found to have a linear behaviour, showing an influence of the spatial resolution on its estimate. The smallest resolution achieved, dx = 0.111 mm, is about 8.5 times the smallest likely Kolmogorov length scale ($\eta \cong 13$ μm) and about 3 times the mean Kolmogorov length scale ($\eta \cong 37$ μm). The ratio between dx and η is of great importance for the assessment of the results. Piirto *et al*. (2000) and Saarenrinne *et al*. (2001), studying Taylor micro scales and the energy dissipation, found results very similar to the ones presented in this work. According to their findings the dissipation that can be calculated with PIV is a fraction of the real dissipation value and depends on the spatial resolution expressed as a function of multiples of the Kolmogorov length scale. In particular they found that in order to enable the measurement of 90 % of the actual energy dissipation, the spatial resolution should be around 2η, and to reach 65 %, around 9η. Therefore in the present work, according to their findings, around 80 % of the true ε value in the less turbulent regions and about 65-70 % in the most turbulent areas could be calculated.
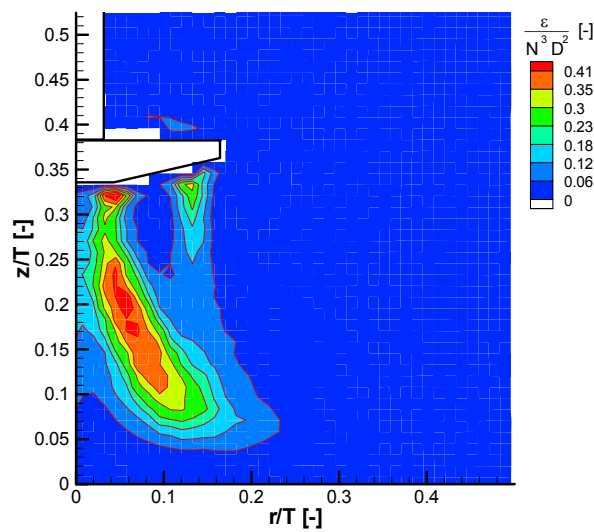

Figure 5 - Contour plot of the normalised turbulence energy dissipation calculated with dimensional relation (1).
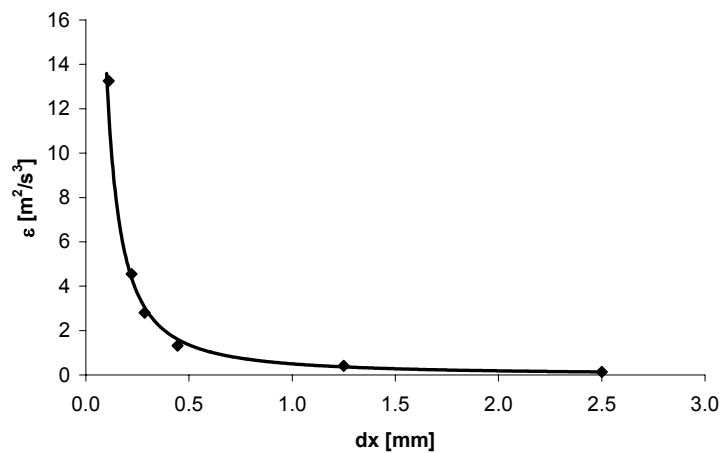

Figure 6 - Turbulence energy dissipation, averaged over the impeller stream region, plotted against spatial resolution of the PIV measurements.

Saarenrinne *et al.* (2001), extending the work of Piirto *et al.* (2000), concluded that the image size of PIV measurements influenced the flow velocity, while the interrogation cell size did not exhibit a clear effect. In the present work a very small dependence of flow velocity over interrogation cell size was found: an increase in velocity value of just 0.006 V_{tip} in the highest velocity region below the impeller was found when changing from dx = 2.5 mm to dx = 0.285 mm, corresponding to an interrogation cell area about 80 times smaller. Such a small change in the velocity values compared to a rather large refinement in the interrogation cell size is not in agreement with the observation of Saarenrinne *et al.* (2001).

4. CONCLUSIONS

Mean flow and turbulence energy dissipation were analysed in a vessel stirred by a hydrofoil impeller. 360° ensemble-averaged measurements were performed. The r.m.s. velocities, skewness, kurtosis and Reynolds stresses were analysed as well. Particular attention was given to the effects of spatial resolution over estimation of energy dissipation. Experiments were performed at spatial resolutions ranging from 2.5 mm to 0.111 mm. The latter was found to be 3 times the vessel-wise average of the Kolmogorov length scale and 8.5 times the smallest Kolmogorov length scale, located in the highest turbulence region below the impeller. Energy dissipation results were compared with findings from other methods (based on dimensional relations) and techniques (LDA). Differences were found and discussed. In particular the dimensional relations were found to be reliable only if the average energy dissipation and its integration over the vessel is considered, but rather incorrect when local ε values and distribution are estimated. Conclusively, the measurement of ε is very difficult with any measurement method but the present work has produced direct measurements of dissipation rate in stirred vessels with PIV and shows much promise for the accurate determination of ε in such flows.

NOMENCLATURE

Roman characters

A	Experimental constant, eq. (1) [-]	
A'	Experimental constant, eq. (3) [-]	
B	Baffle width [m]	
C	Impeller off-bottom clearance [m]	
D	Diameter of the impeller [m]	
H	Total liquid depth in vessel [m]	
K	Turbulent kinetic energy [m^2/s^2]	
	Wave number, eq. (4) [m^{-1}]	
L	Integral length scale [m]	
N	Number of samples [-]	
	Impeller speed [revolutions per second: rps]	
P_o	Impeller power number [-]	
Q	Turbulent kinetic energy, eq. (3) [m^2/s^2]	
R	Radial distance from the axis of the vessel [m]	
	Radial co-ordinate of the measuring volume [m]	
Re	Reynolds number	
T	Diameter of the vessel [m]	
U'_z, u'_r, u'_φ	Axial, radial and tangential r.m.s. velocities [m/s]	
u_z, u_r, u_φ	Axial, radial and tangential fluctuating velocities [m/s]	
U_z, U_r, U_φ	Axial, radial and tangential instantaneous velocities [m/s]	
$\overline{U}_z, \overline{U}_r, \overline{U}_\varphi$	Axial, radial and tangential mean. velocities [m/s]	
V_{tip}	Velocity of the tip of the impeller blades [m/s]	
Z	Vertical co-ordinate of the measuring volume [m]	

Greek characters

Λ_x	Integral length scale, eq. (6) [m]
ε	Turbulence energy dissipation rate [kJ/kg/s]

$\bar{\varepsilon}$	Turbulence energy dissipation rate averaged over the whole vessel [kJ/kg/s]
ε^{*}	Non-dimensionalised turbulence energy dissipation, $\varepsilon/(N^{3}D^{2})$ [-]
η	Kolmogorov length scale [μm]
φ	Tangential co-ordinate of the impeller revolution [deg]
λ	Taylor micro scale [mm]
μ	Dynamic viscosity [kg/m/s]
ν	Kinematic viscosity [m^2/s]
θ	Tangential co-ordinate of the measuring volume [deg]
ρ	Density [kg/m^3]

Abbreviations

2D	Two dimensional
dx	Grid vector spacing, spatial resolution [m]
LDA / LDV	Laser Doppler Anemometry/Velocimetry
PIV	Particle Image Velocimetry
r.m.s.	Root mean square

REFERENCES

Cutter, L.A. (1966). Flow and turbulence in a stirred tank. AICHE J., Vol. 12, pp. 35-45.

Fentiman, N.J., Hill, N.ST., Lee, K.C., Paul, G.R. and Yianneskis, M. (1998). A novel profiled blade impeller for homogenization of miscible liquids in stirred vessels. Trans.I.Chem.E., Vol. 76, part A, pp. 835-842.

Fentiman, N.J., Lee, K.C., Paul, G.R. and Yianneskis, M. (1999). On the trailing vortices around hydrofoil impeller blades. Trans.I.Chem.E., Vol. 77, part A, pp. 731-740.

Hinze, J.O. (1975). Turbulence. New York. McGraw-Hill.

Jaworski, Z. and Fort, I. (1991). Energy dissipation rate in a baffled vessel with pitched blade turbine impeller. Collection of Czechoslovak Chemical Communications, Vol. 56, pp. 1856-1867.

Kresta, S. (1998). Turbulence in stirred tanks: anisotrpic, approximate and applied. Can. J. Chemical Engineering, vol. 76, pp. 563-576.

Kresta, S. and Wood, P.E. (1993). The flow field produced by a pitched blade turbine: characterisation of the turbulence and estimation of the dissipation rate. Chemical Engineering Science, Vol. 48, pp. 1761-1774.

Lee, K., C. and Yianneskis, M. (1998). Turbulence properties of the impeller stream of a Rushton turbine. AIChE journal, Vol. 44, No. 1, pp. 13-24.

Piirto, M., Eloranta, H. and Saarenrinne, P. (2000). Interactive software for turbulence analysis from PIV vector data. 10th International Symposium on Applications of Laser Techniques to Fluid Mechanics, Lisbon.

Pope, S. (2000). Turbulent flows. Cambridge University Press.

Saarenrinne, P. and Piirto, M. (2000). Turbulent kinetic energy dissipation rate estimation from PIV velocity vector fields. Experiments in Fluids, Suppl., pp. S300-S307.

Saarenrinne, P., Piirto, M. and Eloranta, H. (2001). Experiences of turbulence measurement with PIV. Measurement Science and Technology, vol. 12, pp. 1904-1910.

Schäfer, M., Yianneskis, M., Wächter, P. and Durst, F. (1998). Trailing vortices around a 45˚ pitched blade impeller. American Institute of Chemical Engineers Journal, Vol. 44, No. 6, pp. 1233-1246.

Sharp, K.V., Kim, K.C. and Adrian, R.J. (1998). Dissipation estimation around a Rushton turbine using particle image velocimetry. Proc. 9th Int. Symposium on Applics.. of Laser Techniques to Fluid Mechanics, Lisbon.

Sheng, J., Meng, H. and Fox, R.O. (2000). A large eddy PIV method for turbulence dissipation rate estimation. Chemical Engineering Science, Vol. 55, pp. 4423-4434.

Stoots, C., M. and Calabrese, R., V. (1995). Mean velocity field relative to a Rushton turbine blade. AIChE Journal, Vol. 41, pp. 1-11.

Wernersson, E., SW. and Tragardh, C. (1999). Scale-up of Rushton turbine-agitated tanks. Chemical Engineering Science, Vol. 54, pp. 4245-4256.

Yianneskis, M. and Whitelaw, J.H. (1993).On the structure of the trailing vortices around Rushton turbine blades. Transactions of the Institution of Chemical Engineers, Chemical Engineering Research and Design, Vol. 71, pp. 543-550.

Yianneskis, M., Popiolek, Z. and Whitelaw, J.H. (1987). An experimental study of the steady and unsteady flow characteristics of stirred reactors. Journal of Fluid Mechanics, vol. 175, 1987, pp. 537-555.

Zhou, G. and Kresta, S., M. (1996a). Distribution of energy between convective and turbulent flow for three frequently used impellers. Trans. I.Chem.E., Vol. 74, part A, pp. 379-389.

Zhou, G. and Kresta, S., M. (1996b). Impact of tank geometry on the maximum turbulence energy dissipation rate for impellers. AIChE journal, Vol. 42, No. 9, pp. 2476-2490.